 CMC, vol.5, no.1, pp.11-29, 2007

Mechanics of Elastomer–Shim Laminates

A. H. Muhr[1]

Abstract: The mechanics of laminates of elastomer and shims of high modulus material are reviewed. Such structures are often built to provide engineering components with specified, and quite different, stiffnesses in different modes of deformation. The shims may either be rigid or flexible, flat or curved, but are usually close to inextensible, being made of a high modulus material such as steel. On the other hand, rubber has an exceptionally low shear modulus, about one thousandth of its bulk modulus, so that shear of the rubber layers and flexure of the high modulus layers (if thin) are the dominant mechanisms of deformation of the composite. In comparison, extension of the layers and changes to their separation are highly constrained.

Modes of failure are addressed as well as force-deformation behaviour. For compression normal to the laminations, the shear in the rubber results in in-plane tension in the shims, possibly leading to tensile failure. For tension normal to the laminations, the elastomer can cavitate, which would relieve the shear in it and hence the in-plane compressive stress applied to the shim. In flexure, shear in the rubber can apply in-plane compressive stress to the shims and cause buckling failure.

Keyword: Rubber, shape factor, laminates, instability, buckling, cavitation, fracture, damping.

1 Introduction

Rubber is a significant engineering material in its own right, and many interesting aspects of the mechanical characteristics of rubber composites with shims, cords and filler particles have been intensively investigated over the years. Such "reinforcement" is used in rubber to increase its stiffness, often anisotropically by intention, and its load bearing capacity. Two alternative approaches are used to describe the characteristics of the rubber-reinforcement composite: detailed solutions to problems with prescribed geometry, or approximations of the global characteristics, based for example on weighted averages of the constituent properties, finite element simulations of representative volume elements of the composite, or empirical equations. The second approach usually aims to generate the parameters in an elastic continuum model of the composite, in general anisotropic.

It has been pointed out by Spencer [1972] that classical anisotropic elasticity theory can be unsuitable for describing the mechanical properties of cord-rubber composites, because of the near-incompressibility of the rubber and near-inextensibility of the cords. This means that the cords can "channel" stress from one point to a far distant point, in conflict with St Venant's principle and hence with continuum elasticity theory.

Thus the first approach – detailed solutions for prescribed geometries - is valuable wherever the problems are tractable. It has the merit of providing not only stiffnesses, but also details of local stresses in the two materials forming the composite, and hence giving insight into failure. For example, despite its very low shear modulus, rubber pads used as cushions between concrete surfaces can generate large enough tensile stresses in the concrete to crack it [Coveney, Fuller & Muhr, 1989]. The solutions that have been derived for such systems may act as models for mechanisms that could be significant in composite materials at different scales. Rubber-based macro-composites use either cords or shims as the reinforcement; this paper serves to collate work on the mechanics of rubber-shim composites. Some of this work has not previously been published.

[1] TARRC, Brickendonbury, Hertford, SG13 8NL, UK

By "shim" we mean a material with a much higher modulus than rubber, formed such that two of its dimensions are much greater than the third dimension (the thickness). The shims may be either flat or dished, rigid or flexible.

The analysis will be linear, despite the fact that rubber can undergo very large elastic strains and so it is normal to use non-linear finite element packages for modelling rubber components. Historically, however, classical elasticity theory has been found to be very useful for rubber-shim composites. The approach has the merits of (1) analytical tractability (2) delivering relatively simple analytical formulae which at the very least serve the useful purpose of predicting the stiffnesses for small deflections, and, if experience shows the non-linearity is not great, extrapolate to make useful approximate predictions at larger deformations. In fact extrapolation to large deformations is reasonably reliable, because the shims constrain the mode of straining of rubber to be predominantly simple shear, and this mode has nearly linear stress-strain behaviour, at least for unfilled rubber.

2 Mechanics Of Rubber Laminates With Rigid Shims

2.1 General form of equations for describing the force-deflection behaviour of an elastic component

We seek a set of linear constitutive rules describing the forces and moments required to achieve the usual six spatial degrees of freedom of motion of a rigid shim, bonded to a layer of rubber, relative to a reference point, the adjacent shim being regarded as fixed in position.

The constitutive rules will give the relationship between a generalised relative displacement vector **x**, consisting of three translation components (in the x, y and z directions) and three rotational components (about the x, y and z axes), and the equivalently generalised force vector **f**. Assuming linearity, the rules may be written as a matrix equation

$$\mathbf{f} = \mathbf{K}\mathbf{x} \tag{1}$$

where **K** is a 6×6 matrix of stiffnesses. Translations are free vectors, whereas rotations require not only the angle of rotation and the direction of the axis of rotation to be defined, but also the position of the axis of rotation. Force is a positioned vector, and may be resolved into a force of the same magnitude and direction acting on a chosen point, and a couple, given by the moment of the force (acting at its original position) about the chosen point. To define **x** and **f** unambiguously not only the directions of the coordinate axes need to be defined, but also their origin, which is taken to be the point of application of **f** as well as the point through which the rotation axes pass. One of the shims (the moving one) together with this point of application may be considered to comprise a rigid body, which is displaced by **x** relative to the other shim under the action of **f**. This implies that the diagonal terms K_{11}, K_{22} and K_{33} depend only on the directions of the coordinate axes, whereas the remaining terms also depend on the point of application (the origin). In any case, following Schapery & Skala [1976], we can say that **K** is symmetric to be consistent with a strain energy function U for the rubber:

$$K_{ij} = \frac{\partial U}{\partial x_i \partial x_j} = \frac{\partial U}{\partial x_j \partial x_i} = K_{ji} \tag{2}$$

If **x** is chosen to be a simple displacement parallel to an axis of symmetry, the resultant **f** will be coaxial with it. If there are three orthogonal axes of symmetry with a common inter-section (centre of rigidity), and a coordinate system is chosen to be coaxial with them and with the origin at the intersection, then **K** will be diagonal. The centre of rigidity has the property that a force acting in line with it results in a coaxial displacement, and no rotation. Equivalently, a couple produces a coaxial rotation about the centre of rigidity, and no displacement of it.

2.2 Derivation of constitutive equations for a planar laminar element

Consider now a disc of rubber of radius a and thickness h bonded between two flat rigid discs, with $h << a$ (Fig. 1).

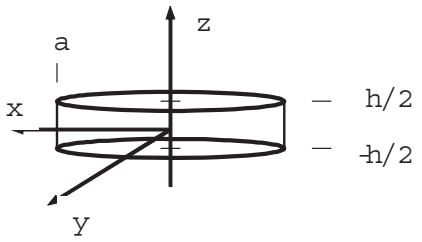

Figure 1: Disc of rubber bonded between two shims

The centre of rigidity coincides with the geometric centre of the laminate, and this will be taken as the centre of coordinates. Thus **K** will be diagonal and we shall use just one index to denote its six components. The rubber will, to first approximation, deform by shearing parallel to the shims; the bond prevents lateral slip at the boundary. For deflection in the x and y directions the strain will be nominally homogenous simple shear, whereas for torsion about the z axis the shear strain is in the circumferential direction and proportional to the distance from the z-axis, leading to:

$$K_1 = K_2 = \frac{\pi G a^2}{h} \tag{3}$$

$$K_6 = \frac{\pi G a^4}{2h} \tag{4}$$

Strictly speaking , the right-hand side of Eq.(3) is an upper bound for the left, because the boundary condition of zero shear strain on the free rubber surface (a small area) is not met. However, for $a >> h$, it is a tight upper bound (Gregory & Muhr, 1999). On the other hand, Eq.(4) is the exact solution, despite the strain field being non-uniform.

Deflection parallel to the z-axis will involve a more complicated distribution of simple shear strain. Following Rocard [1937], we could guess a displacement field u that meets the requirements that $u_r = 0$ at $z = \pm h/2$, $u_z = 0$ at $z = 0$ and the total volume is constant:

$$\begin{aligned}
u_z &= \frac{3}{2} ez \left(1 - \frac{4z^2}{3h^2}\right) \\
\Rightarrow e_z &= \frac{\partial u_z}{\partial z} = \frac{3}{2} e \left(1 - \frac{4z^2}{h^2}\right) \\
u_r &= -\frac{3}{4} er \left(1 - \frac{4z^2}{h^2}\right) \\
\Rightarrow e_r &= \frac{\partial u_r}{\partial r} = -\frac{3}{4} e \left(1 - \frac{4z^2}{h^2}\right) \\
\gamma_{rz} &= \left(\frac{\partial u_r}{\partial z} + \frac{\partial u_z}{\partial r}\right) = \frac{6erz}{h^2}
\end{aligned} \tag{5}$$

where $e = \frac{u_z(h/z)}{h/z}$ is the average compressive strain.

According to the Ritz methd, an upper bound for the compression stiffness K_3 may be obtained from the total energy associated with this strain field:

$$\begin{aligned}
\frac{1}{2} K_3 (eh)^2 &< G \int_{-h/2}^{h/2} \int_0^a (2e_r^2 + e_z^2 + \gamma_{rz}^2) 2\pi r \mathrm{d}r \mathrm{d}z \\
\Rightarrow K_3 &< \frac{3\pi a^2 G}{h} \left(\frac{6}{5} + 2S^2\right) \approx \frac{6\pi a^2 G S^2}{h}
\end{aligned} \tag{6}$$

where S, the "shape factor", is given by

$$S = \frac{\text{area of loaded face}}{\text{area of rubber free to bulge}} = \frac{a}{2h} \tag{7}$$

It is known [Coveney, Fuller & Muhr, 1989; Rocard, 1937; Gent & Meinecke, 1970] that Eq. (6) is rather a tight upper bound, so that for engineering purposes it may be taken as an equality if $3 < S < 10$. Yeoh (1985) has provided a suitable equation for $0 < S < 0.5$. For $0.5 < S < 3$ the approximate form of Gent & Lindley (1959) with 1, rather than 6/5, added to the term in brackets on the right hand side of Eq. (6) is adequate. For higher values of S it is necessary to include the effect of compressibility of the rubber, as discussed later in this section.

Similarly, for a tilt of $\theta/2$ of each endplate about the y-axis we can guess the following displace-

ment field:

$$
\begin{aligned}
u &= \frac{3\theta}{16h}\left(1-\frac{4z^2}{h^2}\right)\left(3x^2+y^2-a^2\right)\\
&\Rightarrow e_1 = \frac{9\theta x}{8h}\left(1-\frac{4z^2}{h^2}\right)\\
v &= \frac{3\theta xy}{8h}\left(1-\frac{4z^2}{h^2}\right)\\
&\Rightarrow e_2 = \frac{3\theta x}{8h}\left(1-\frac{4z^2}{h^2}\right)\\
w &= -\frac{3\theta xz}{2h}\left(1-\frac{4z^2}{3h^2}\right)\\
&\Rightarrow e_3 = -\frac{3\theta x}{2h}\left(1-\frac{4z^2}{h^2}\right)\\
&\Rightarrow \gamma_{12} = \frac{\partial u}{\partial y}+\frac{\partial v}{\partial x} = \frac{3\theta y}{4h}\left(1-\frac{4z^2}{h^2}\right)\\
&\Rightarrow \gamma_{13} = \frac{\partial u}{\partial z}+\frac{\partial w}{\partial x}\\
&= -\frac{3\theta z}{2h^3}\left\{3x^2+y^2-a^2+h^2(1-\frac{4z^2}{3h^2})\right\}\\
&\Rightarrow \gamma_{23} = \frac{\partial v}{\partial z}+\frac{\partial w}{\partial y} = -\frac{3\theta xyz}{h^3}
\end{aligned}
\tag{8}
$$

and arrive at the upper bound:

$$
\begin{aligned}
\frac{1}{2}K_5\theta^2 &< G\iiint\{(e_1^2+e_2^2+e_3^2)\\
&\qquad +\frac{1}{2}(\gamma_{12}^2+\gamma_{13}^2+\gamma_{23}^2)\}\mathrm{dxdydz}\\
\Rightarrow K_5 &< \frac{\pi G a^2}{h}\left(\frac{S^2a^2}{2}+\frac{21a^2}{20}+O(h^2)\right)\\
&\approx \frac{\pi G S^2 a^4}{2h}
\end{aligned}
\tag{9}
$$

Thus the stiffness matrix for the laminate is

$$
\mathbf{K} \approx \frac{\pi a^2 G}{h}\begin{pmatrix}
1 & 0 & 0 & 0 & 0 & 0\\
0 & 1 & 0 & 0 & 0 & 0\\
0 & 0 & 6S^2 & 0 & 0 & 0\\
0 & 0 & 0 & \frac{S^2a^2}{2} & 0 & 0\\
0 & 0 & 0 & 0 & \frac{S^2a^2}{2} & 0\\
0 & 0 & 0 & 0 & 0 & \frac{a^2}{2}
\end{pmatrix}
\tag{10}
$$

Some of the components of **K** are larger than others by a factor of S^2, so that the stiffness is strongly anisotropic. This is exploited in many designs of rubber engineering components. The reason for the upper bound values to become too loose to be good estimates for the stiffnesses is that if $S > 10$ then the contribution of bulk compression K of the rubber to the total deflection can no longer be regarded as negligible, the bulk modulus of rubber being about 2000MPa; the criterion could instead be expressed as $GS^2 << K$.

More insight may be gained by considering the stresses within the rubber layer. Consider an elemental column of the material of cross section δx. δy running from z = -$h/2$ to $z = h/2$. The shear stresses required to bow the column will be balanced by a pressure p within the rubber, giving:

$$
\frac{\partial p}{\partial x} = -G\frac{\partial^2 u}{\partial z^2}; \quad \frac{\partial p}{\partial y} = -G\frac{\partial^2 v}{\partial z^2} \tag{11}
$$

$$
\Rightarrow \frac{\partial^2 p}{\partial x^2}+\frac{\partial^2 p}{\partial y^2} = -G\frac{\partial^2}{\partial z^2}\left(\frac{\partial u}{\partial x}+\frac{\partial v}{\partial y}\right) \tag{12}
$$

Preservation of the volume of the element gives:

$$
2w(h/2) = \int_{-h/2}^{h/2}\left(\frac{\partial u}{\partial x}+\frac{\partial v}{\partial y}\right)\mathrm{dz} \tag{13}
$$

Combining Eqs. (11) and (12), and assuming that p is independent of z, or, equivalently, that the bulge profiles are parabolic in z, gives [Gent & Meinecke (1970), Adkins (1954)]:

$$
\frac{\partial^2 p}{\partial x^2}+\frac{\partial^2 p}{\partial y^2} = -\frac{24Gw(h/2)}{h^3} \equiv \frac{12Ge}{h^2} \tag{14}
$$

By solving Eq. (14) we may find the pressure distribution in the rubber, and the shear stresses on the shims may then be found by integrating Eq. (11). These stress distributions may be integrated to give the total forces on the shims, and also used to calculate the local stresses in the shims. Gent, Henry & Roxbury (1974) confirmed the parabolic pressure distribution across a compressed bonded pad experimentally.

For the case of compression of the disc p is found to be

$$
p = \frac{12S^2Ge}{a^2}(a^2-x^2-y^2) \tag{15}
$$

For the case of tilting about the y-axis, p is found to be

$$
p = \frac{12S^3G\theta x}{a^3}(x^2+y^2-a^2) \tag{16}
$$

Chalhoub and Kelly [1990] have generalised equation (14) to include the compressibility of the rubber; e on the right hand side is simply replaced by $e-(p/K)$, representing the fractional loss in volume of the element due to the movement together of the shims, less that due to bulk compression, which determines the rate of increase in the bulge as x and y are increased. Papoulia & Kelly [1996] have shown that this generalized equation may also be obtained from the Hellinger-Reissner variational principle. A cruder way of taking bulk compression into account, for estimates of the stiffness of the laminate, is to add the compliances from the incompressible case and the case of uniform bulk compression [Gent & Lindley, 1959].

2.3 Constitutive equations for a spherical laminar element

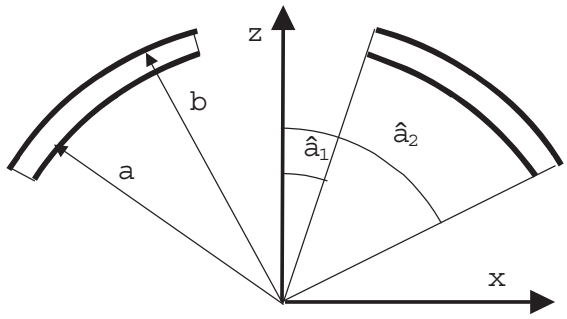

Figure 2: Section in xz plane through a spherical laminar element (z is the axis of revolution)

The theory for planar laminates has been motivated by their application as bridge bearings, antivibration bearings for buildings and seismic isolation bearings, and an extensive literature exists on mathematical expressions describing their force-deformation behaviour. Similar laminates, but with spherically dished shims, are used for rocket thrust nozzles, helicopter rotor bearings and flexjoints for offshore oil platforms, but most work on their mechanics had been expounded only in company reports until recently [Baumann, 2005].

A spherical laminar element is shown in Fig. 2; it is a portion of a full sphere, as is typical, limited by angles β_1 and β_2. Because it is only a portion, it has only one axis of symmetry, taken here as the z-axis. Modes of deformation are most easily described taking the origin of the axes to coincide with the centre of the sphere through the centre of the rubber layer, having radius c. Then the Ritz approach, and assumption of incompressibility, leads to the following stiffness matrix:

$$\mathbf{K} \approx \frac{\pi c^4 G}{h} \begin{pmatrix} \frac{\alpha_1^3}{h^2} & 0 & 0 & 0 & \frac{\alpha_2}{c} & 0 \\ 0 & \frac{\alpha_1^3}{h^2} & 0 & \frac{\alpha_2}{c} & 0 & 0 \\ 0 & 0 & \frac{\alpha_4}{h^2} & 0 & 0 & 0 \\ 0 & \frac{\alpha_2}{c} & 0 & \alpha_1+\frac{\alpha_3}{3} & 0 & 0 \\ \frac{\alpha_2}{c} & 0 & 0 & 0 & \alpha_1+\frac{\alpha_3}{3} & 0 \\ 0 & 0 & 0 & 0 & 0 & \alpha_1-\frac{\alpha_3}{3} \end{pmatrix} \tag{17}$$

where

$$\begin{aligned} c &= a+\frac{h}{2} = b-\frac{h}{2} \\ \alpha_1 &= \cos\beta_1 - \cos\beta_2 \\ \alpha_2 &= \cos^2\beta_1 - \cos^2\beta_2 \\ \alpha_3 &= \cos^3\beta_1 - \cos^3\beta_2 \\ \alpha_4 &= 4\alpha_3 \\ &\quad + \frac{6\{\alpha_1\alpha_5+\alpha_2[\cos\beta_2 \ln(\tan\frac{\beta_1}{2})-\cos\beta_1\ln(\tan\frac{\beta_2}{2})]\}}{\ln(\tan\frac{\beta_2}{2})-\ln(\tan\frac{\beta_1}{2})} \\ \alpha_5 &= \int_{\beta_2}^{\beta_1} \sin 2\theta \ln(\tan\frac{\theta}{2}) d\theta \end{aligned} \tag{18}$$

In Eq. (17) the derivation of K_{66} has been provided by Baumann [2005] whereas the other coefficients were originally derived by Schapery [see 2006] who also provided solutions for the nearly incompressible case. It is apparent from Eq. (17) that the translational stiffnesses are all subject to the shape factor effect, because of the curvature of the laminate, whereas the rotational stiffnesses are not, because the origin of the coordinate axes coincides with the centre of curvature. Schapery [see 2006] started with physically reasonable displacement fields, satisfying boundary conditions and containing unspecified constants and functions, as in the Ritz method. However, he did not

evaluate the unknowns by minimization of strain energy, so the derived stiffnesses do not have the status of strict upper bounds. Complete evaluation of the strain energy integral is very involved, as may be appreciated even for the relatively simple case of Eq. (9). Instead, Schapery simplified the problem by neglecting terms of second order in h/a, and derived forces and moments by integrating stresses over surfaces, rather than from the energy. In any case, this is necessary for calculating the off diagonal elements of **K**.

3 Mechanics of Beam-columns of Laminates

3.1 Theory

In order to make a component with, for example, a very high compression stiffness and a low shear stiffness, rubber laminates are often manufactured together in a stack. For sufficiently low loads the compliances may be calculated by adding the compliances of the individual layers. However, at higher loads the internal degrees of freedom result in an effect of axial load on lateral stiffness, and at sufficiently high axial load the bearing can become unstable, the lateral stiffness falling to zero. This behaviour, akin to buckling of an Eulerian strut but taking into account the very low shear stiffness and high bending stiffness, can be understood from an appropriate beam-column theory [Gent, 1964; Schapery & Skala, 1976; Thomas, 1983].

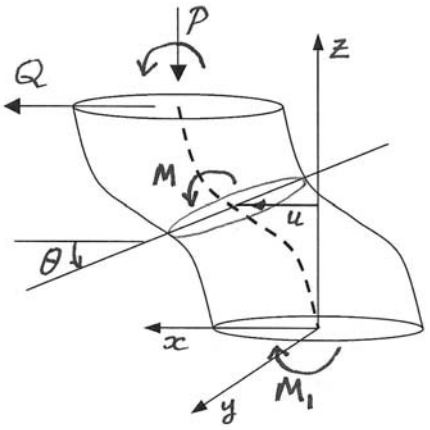

Figure 3: Beam-column with θ (orientation of shims) as internal variable

The laminated beam-column is treated as a continuum, with the stiffnesses calculated as in section 2.2 smeared out, so that the beam has stiffnesses of unit length of K_{ij}(t+h), where t is the thickness of a shim, and so (t+h) is the length of the column taken up by one layer of rubber and one shim. Following Schapery & Skala [1976], we may consider the axial load P to be first applied, and the length L, and bending and shear stiffnesses of unit length to be functions of P but otherwise the analysis to be linear. At any position z along the axis of the column a cross section is acted on by the forces P and Q, and the moment M (Fig. 3). The objective is to find the lateral deflection u of the centreline as a function of z, and to estimate the local stresses throughout the beam. The angle θ that the shims make to the x-axis is an internal variable. The profile du/dz of the beam is related kinematically to θ and the shear strain γ by

$$\text{kinematics: } \frac{\mathrm{d}u}{\mathrm{d}z} = \gamma\cos\theta + \sin\theta \approx \gamma + \theta \qquad (19)$$

In the absence of body forces, P and Q are independent of z, but M varies according to

$$\text{static equilibrium: } M = M_1 - Pu - Qz \qquad (20)$$

where M_1 is the value at $z = 0$. Schapery & Skala [1976] developed equations for $M(z)$; note that $u(z)$ may readily be found from $M(z)$ using Eq. (20) and the boundary conditions. Eqs. (19) to (28) summarise Schapery & Skala's theory [1976] which is generalised from earlier publications [eg Gent, 1964] and includes the possibility that **K** is not diagonal (eg for dished shims).

The constitutive equations are:

$$\text{moments: } M = B\frac{d\theta}{dz} + A\left(\frac{du}{dz} - \theta\right) \equiv B\theta' + A(u' - \theta) \qquad (21)$$

where

$$B = K_{55}(t+h); \quad A = K_{15}(t+h) = K_{51}(t+h)$$

$$\text{shear: } Q + P\theta = R\gamma + A\theta' \quad \text{where } R \equiv K_{11}(t+h) \qquad (22)$$

Using Eq. (19) to eliminate γ from Eq. (22) gives

$$Q + P\theta = R\left(u' - \theta\right) + A\theta' \tag{23}$$

Eliminating u' from Eqs. (21) and (23) leads to

$$\begin{aligned} &RM = AQ + AP\theta + D\theta' \\ &\text{where } D \equiv BR - A^2 \end{aligned} \tag{24}$$

Eliminating u' from Eqs. (20) and (23) gives

$$RM' = -P\{Q + (P+R)\theta - A\theta'\} - QR \tag{25}$$

Eliminating θ' from Eqs. (24) and (25) and differentiating gives

$$APM' - DM'' = P\{BP + D\}\theta' \tag{26}$$

Eliminating θ from Eqs. (24) and (25) gives

$$(P+R)M + AM' = (PB + D)\theta' \tag{27}$$

Eliminating θ' from Eqs. (26) and (27) leads finally to:

$$\begin{aligned} &M'' + q^2 M = 0 \\ &\text{where } \mathrm{q}^2 = \frac{P(P+R)}{D} \end{aligned} \tag{28}$$

Solutions of Eq. (28) involve trigonometric functions of qz. In the case of flat, rigid shims and high axial stiffness, it may be shown that [eg Thomas, 1983] the lateral stiffness of a laminated bearing of active height L with the end plates constrained to be horizontal (the usual case for seismic isolation bearings) is given by

$$K_s = \frac{Q}{u(L)} = \frac{P^2}{2qB\tan(qL/2) - PL} \tag{29}$$

It follows from equation (29) that the lateral stiffness falls monotonically as P is increased, reaching zero for a critical load given by Eq. (30):

$$P_{crit} = \frac{R}{2}\left\{\sqrt{1 + \frac{4\pi^2 B}{RL^2}} - 1\right\} \approx \frac{\pi}{L}\sqrt{RB} \tag{30}$$

The approximate form of Eq. (30) shows that if the thickness t of the shims is changed there is very little effect on the buckling load, since R, B and L are all proportional to $h + t$.

Another important prediction is that the height of the bearing will drop according to the square of the lateral deflection [Thomas, 1983]. Neglecting axial compliance, this follows from the analogue for w of Eq. (19):

$$\frac{dw}{dz} = -\gamma\sin\theta + 1 - \cos\theta \approx -\frac{\theta^2}{2} - \theta\gamma \tag{31}$$

3.2 Experimental

An extension of a previous experimental study by Gregory & Muhr (1995) was undertaken, using the same bearing geometry but a material with simpler stress-strain behaviour to simplify interpretation of the results.

Cylindrical bearings were made at TARRC from unfilled natural rubber (EDS19 formulation given by TARRC [1979 - 1986]) and mild steel reinforcing shims and endplates. The bearings were assembled from unvulcanised calendered rubber sheet, and metal inserts coated with the Chemlok 205/220 bonding system. A pin of 10mm diameter was inserted through close fitting central holes in the endplates, unvulcanised calendered rubber sheet and metal inserts coated with the Chemlok 205/220 bonding system. A pin of 10mm diameter was inserted through close fitting central holes in the endplates, unvulcanised calendered rubber sheet and shims, and the mould endplates, to prevent lateral displacement. The assembly was cured in a press for a sufficient time to ensure complete vulcanization throughout.

Details of the internal construction of the bearings are given in Table 1. Single shear tests were conducted on one of each bearing type. Dynamic strain amplitudes of 100% (or 50% in the case of zero load) were applied at 0.5Hz and the shear force and deflection were logged for a range of fixed loads, up to the level at which the slope of the load-deflection plot at the origin becomes negative. Two hundred data points were captured for each cycle.

It was noted that as the normal load is increased, the hysteresis increases. Since the theory does not include hysteresis, the underlying force-deformation behaviour was extracted from the hysteresis loops by constructing the "skeleton

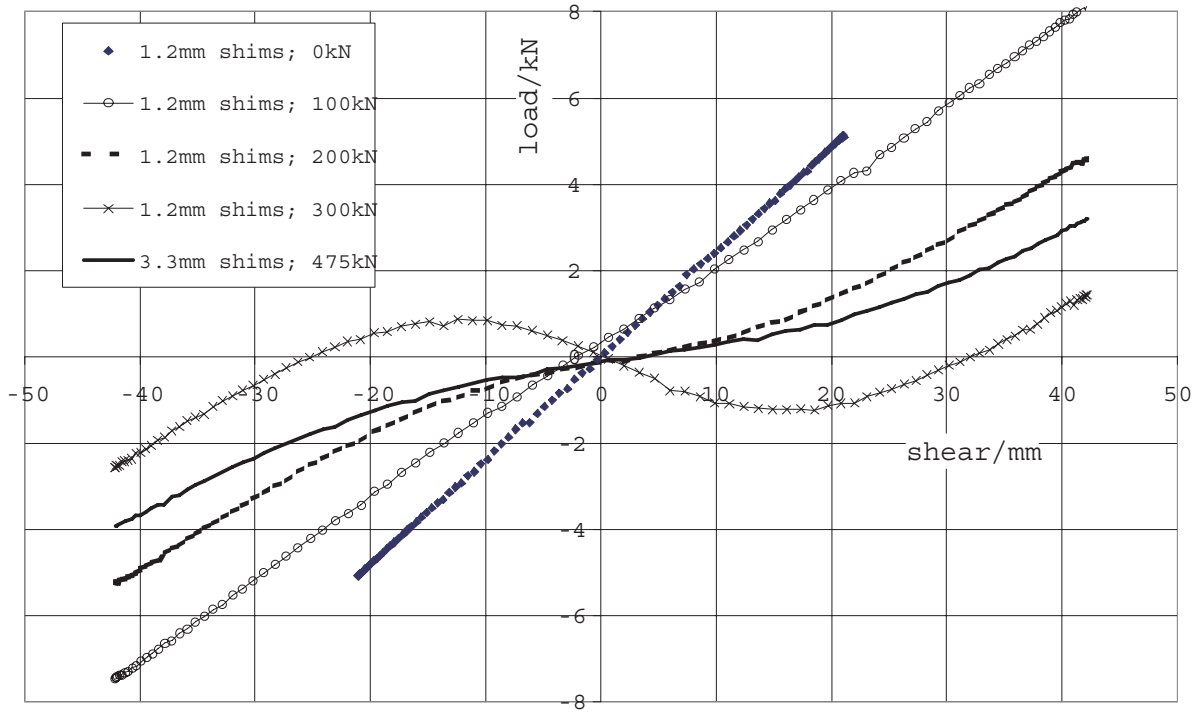

Figure 4: Selected third cycle skeleton load-deflection curves for the bearings

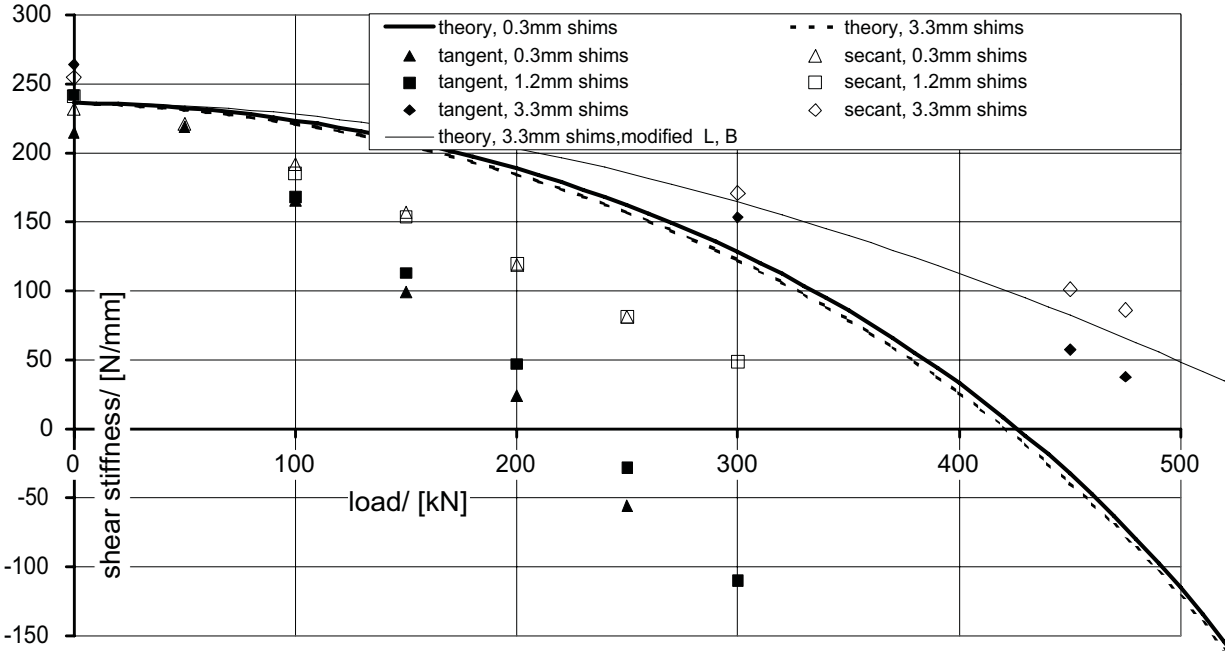

Figure 5: Dependence of shear stiffnesses on normal load (third cycle, 100% shear strain loops)

Table 1: Construction of test bearings

Number of layers (n)	15
Rubber thickness (h)	2.8mm
Plate diameter (2a)	140mm
Plate thickness (t)	0.3, 1.2 and 3.3mm
Hole diameter	12mm
Cover layer thickness (Δa)	4.5mm
S	12.5
Endplates (ΔL)	20mm, tapped

curve" from the mean of pairs of points on the "extension" and "retraction" branches of the loops corresponding (approximately) to the same shear deflection [Ahmadi & Muhr, 1997]. The skeleton curves show progressively more non-linear behaviour as the normal load is increased (see Fig. 4). For comparison of the experimental data with the linear beam-column theory it is necessary to linearise the data by extracting a single stiffness value. Two methods of linearization were applied: the tangent stiffness of the skeleton curve at zero shear, and the secant stiffness at maximum shear, the latter being the same whether the skeleton curve or the full loop is used. The tangent stiffness was found by the "trendline" regression fit in Excel to the 8 data points of the skeleton curve nearest to zero shear, corresponding to a range of about +/- 5mm.

Fig. 5 compares the shear stiffnesses calculated in this way with the linearised theory. It shows that the shear stiffness for all three bearings is approximately 250N/mm for no normal load. To fit this to the geometry given in Table 1 required a value of 0.57MPa for G, about 10% higher than expected for the material. The theoretical curves in Fig. 5 are constructed using this value, and 2000MPa for K. They ignore the presence of the central hole; it will reduce the axial stiffness, [Gent, 1994; Yeoh, 2002] and also the tilting stiffness and hence B. It is thus rather surprising that the theory underestimates the stability of the bearing with the thickest shims, since it will be nearest to the assumption of rigidity of the shims. The reason is believed to be that B increases significantly as the normal load is increased, as found by Gregory & Muhr's [1995] plane strain FEA study. Schapery & Skala [1976], and Stanton, Scroggins, Taylor & Roeder, [1990], have suggested that allowing for the reduction in L by the axial compression as the load increases can significantly increase stability. This is a more potent effect, assuming B and R are unaffected, than simply that of the decrease in L brought about by using thinner shims, since t and $(qL/2)$ will hardly change in the latter case because consequent changes to B and R will largely cancel the decrease in L (see discussion after Eq. (30)). Furthermore, taking into account that B will rise if the plates come closer together [Schapery & Skala, 1976; Stanton, Scroggins, Taylor & Roeder, 1990; Gregory & Muhr, 1995] together with the reduction in L can plausibly explain the discrepancy between theory and experiment for the bearing with 3.3mm shims. If B in Eqs. (28) and (29) is replaced by $B/(1-P/AE_c)^{-3}$ where E_c is an estimate for the compression modulus (eg $6GS^2$), to correct approximately for the reduction in h in the equations used to estimate B, and also L is replaced by $(1-P/AE_c)L$, the modified theory fits the stiffness results better (Fig. 5). In this modified theory, B increases by 29% at 500kN load; and L is reduced by 12%; the two effects make contributions of similar magnitudes to the enhanced stability. Plane strain FEA [Gregory & Muhr, 1995] shows that R decreases slightly with axial load; for the present purposes this effect has been ignored. The improved agreement of the modified theory with the experimental shear stiffnesses for the 3.3mm shims suggests that the non-linearity of the shear load-deflection behaviour could be captured by a further refinement of the theory to include not only the effect of P on B, but also the effect of the relative tilt between adjacent shims on B. Both effects will increase B through the approach of the adjacent shims, effectively increasing the shape factor; however, the second effect will lead to a non-linear differential equation for the profile of the deformed bearing, so that numerical analysis would be necessary to find a solution. A striking feature of Fig. 5 is the nearly identical results for bearings with 0.3 and 1.2mm thick shims, especially for the secant stiffness. This suggests that both shims are effectively close to the "fully flexible" limit, while it

is known that even the thinnest shims may be regarded as inextensible [Gregory & Muhr, 1995].

In their plane strain FEA study, Gregory & Muhr [1995] showed that the transition from "flexible" to "rigid" behaviour of the shims takes place over about a tenfold increase in shim thickness. It would seem from the present results that 3.3mm thick shims are near to the rigid end of this transition.

4 Failure within Laminates with Rigid Shims

4.1 Yielding of shims

Each side of the shim between two compressed rubber layers will be subjected to radial tractions τ which may be calculated from Eq. (5). Taking the thickness t of the shim to be small, the sum of the tractions is equivalent to a body force $2\tau/t$. The problem is then formally identical to that of a spinning disc, the solution for which has been given by Timoshenko and Goodier [1970]:

$$\begin{aligned} &\text{radial stress } \sigma_r = \frac{3+\nu}{8}(a^2-r^2)\mu \\ &\text{hoop stress } \sigma_\theta = \mu\left(\frac{3+\nu}{8}a^2 - \frac{1+3\nu}{8}r^2\right) \\ &\text{where } \mu = \frac{24GS^2eh}{a^2t} \end{aligned} \tag{32}$$

and ν is Poisson's ratio. Taking the third principal stress as the pressure p, given from Eq. (14) by

$$p = \frac{12S^2Ge}{a^2}(a^2-x^2-y^2) \tag{33}$$

we may calculate the von Mises criterion for failure of the shim. This is based on the distortional strain energy density in the general strain state of interest being less than that in uniaxial tension at yield:

$$\sigma_{VM} \equiv \sqrt{\frac{(\sigma_1^2-\sigma_2^2)+(\sigma_1^2-\sigma_3^2)+(\sigma_2^2-\sigma_3^2)}{2}} < \sigma_Y \tag{34}$$

where σ_Y is the yield stress in uniaxial tension. Inserting the maximum stresses from Eqs. (32) and (33), which occur at the centre of the shim, leads to

$$\sigma_{VM} = \left(\frac{3+\nu}{8} - \frac{t}{2h}\right)a^2\mu \approx \frac{3+\nu}{8}a^2\mu \tag{35}$$

4.2 Local shear strain within rubber

Eqs. (5) and (8) quantify the shear strain in the rubber and show that it reaches a maximum at r = a, the bond edge. Failure of the rubber or its bond to the shim cannot be quantitatively related to the shear strain, and catastrophic failure would require very high strains, calling into question the validity of the small strain analysis. Nevertheless, the magnitude of shear strain, calculated according to the small strain theory, is used as a guide for limiting the compression, tilt and shear imposed on laminated bridge bearings (EN 1337 part 3 clause 5.3.3). For such purposes, the linearity of the small strain analysis can be exploited to add the strain contributions for the different modes of deflection of the layer. Small strain analysis actually works remarkably well for laminates, because the rubber is primarily in simple shear and the finite shear stress-strain behaviour of rubber is close to linear.

Fracture mechanics is normally found to be useful for predicting mechanical failure of rubber, but in the region of the bond at the edge of a deformed laminate there is a difficulty. The approximate analysis presented in section 2.2 is inconsistent with the fact that the shear stress and the normal tensile stress must be zero at the free surface of the rubber, and a more detailed analysis shows that there is a stress-singularity where the free and bonded surfaces meet, in the absence of a radiused "fillet". An investigation using finite element analysis has been carried out and has revealed that the behaviour is as if a long crack pre-exists at the bond edge [Lindley & Teo, 1979; Gough & Muhr, 2005], the energy release rate for which may be estimated using the results of section 2.2. For annular cracks of length c propagating inwards from the edge at the bottom and top of a rubber layer in compression, adjacent to the

bond, the energy release rate T is given by

$$T = -\frac{\partial U}{\partial A} = -\frac{\partial U}{\partial c}\left(\frac{d}{dc}2\pi((a^2-(a-c)^2)\right)^{-1} = \frac{-1}{4\pi(a-c)}\frac{\partial U}{\partial c} \tag{36}$$

where U, the total strain energy, may be calculated from the stiffness and the assumption of linearity, for example in compression we would have

$$U_{\text{comp}} \approx \frac{1}{2}K_3(eh)^2 \tag{37}$$

whence, from $K_3 = \dfrac{6\pi G}{h}\dfrac{(a-c)^4}{4h^2}$

$$T_{\text{comp}} = \frac{3G}{4h}(a-c)^2e^2 \equiv \overline{W}_{\text{comp}}h \tag{38}$$

where $\overline{W}_{comp}$ is the total strain energy divided by the volume of rubber in the uncracked region of the rubber layer. The energy release rate in tilting may be estimated in the same way, except that the crack is more likely to develop as a crescent, with little crack growth in the neighbourhood of the axis of rotation.

4.3 Local hydrostatic pressure within rubber

Unfilled rubber cavitates, an elastic instability, if subjected to a hydrostatic tension of theoretically 5*G*/2 [Gent & Lindley, 1958]. This may occur for laminar elements that are put into tension or tilted. In either case the criterion is that the local hydrostatic pressure p, calculated from Eq. (5) or (6) exceeds -5*G*/2. The theory agreed well with experiments of bonded rubber blocks in tension [Gent & Lindley, 1958], so would be expected to work also for blocks in tilt or a combination of tension and tilt.

4.4 Failure in laminar beam-columns

The beam-column theory of Section 3 provides the shear and tilt of each element (the compression is common) and may be used together with the equations for local stresses in the elements to predict stresses throughout the column. We can thus predict where and by what mechanism (shim yield, near-bond cracking of the rubber or cavitation of the rubber) the stack of elements might fail if subjected to a given mode of loading. For example, Thomas calculated the horizontal deflection at which the end layer of a laminated isolation bearing; should suffer from cavitation [Muhr & Thomas, 1991]. It is interesting to note that local hydrostatic tension is expected, even for bearings under high compressive loads, if the shear deflection d is large enough, because the end layer is subjected to a tilting moment given by $M = (QL+Pd)/2$. In experiments on model bearings the deflection at which the effect of cavitation is apparent from the shear load-deflection behaviour is somewhat larger than predicted [Thomas, 1983], possibly because the reduction in tilting stiffness caused by cavitation is not immediately obvious in the load-deflection behaviour of the bearing, but manifests itself only at larger deflections. The model bearings had very thick "shims", but experiment and Finite Element analyses suggest that for typical bearings the shims flex under large shear deflections for typical loads (section 3.2), giving an additional reason for cavitation to be delayed to larger deflections than predicted.

5 Mechanics of Rubber Laminates with Flexible Shims

5.1 Beam-columns comprising stacks of laminar elements with flexible shims

In the previous theory sections, the shims were assumed to be rigid. The thickness of the shims is not generally chosen to ensure this is so, but rather, simply to ensure that the von Mises stress in them (eg Eq. (35)) is less than the yield stress by an appropriate margin. In practice, for compactness, ease of handling and economy, the chosen thickness for the shims is generally little thicker than permitted by this criterion, and flexing of the shims does occur for lateral deflection of the stack. Kelly [1994] has developed a plane strain theory that includes shim flexibility, through an additional internal variable, the amount of warp, as a function of z. It remains to check the predictions of this theory against ex-

periment.

At TARRC theory and experimental validation have been carried out for a different geometrical arrangement of rubber layers bonded between flexible shims. This is described in section 5.2.

5.2 *Mechanics of flexure of a rubber layer bonded between flexible shims*

Muhr & Thomas [1989] developed design equations for novel springs based on flexure of rubber-steel laminates. Since most of the deformation energy is stored in the rubber, the composite springs have the attributes of rubber springs, such as fine control, by choice of elastomer, of stiffness and damping. However, for a specified deflection capacity, much lower design stiffnesses can be met in comparison with conventional rubber springs.

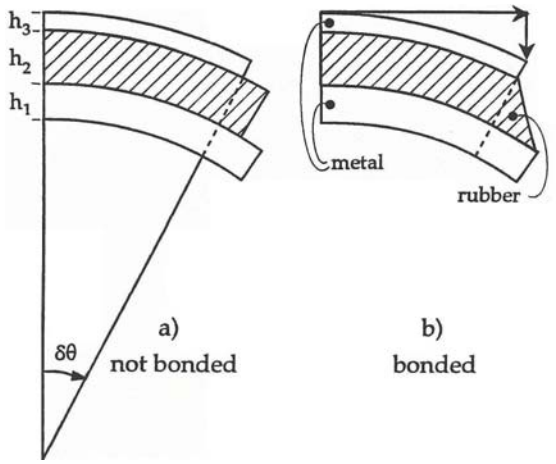

Figure 6: Effect of flexure of a sandwich: layers 1 and 3 have a much higher elastic modulus than layer 2 and are assumed not to change length. Horizontal axis is x, vertical deflection is w, angle increment is $\delta\ \theta$, (a) free slip-page at interface (b) no slippage allowed.

Fig. 6 shows how bonding the rubber to the shims changes its mode of deformation from simple bending, making little contribution to flexural stiffness, to shear, making a significant contribution to beam stiffness. Making the following assumptions:

1. *plane strain*
2. *incompressibility of the rubber*
3. *centre lines of layers 1 and 3 (the shims) do not change length*
4. *radius of curvature* $>> h_1, h_2, h_3$

it follows that the increment δs to the shear deflection of the rubber is related to the increment in the angle of bending $\delta\theta$ by

$$\delta s = \left(h_2 + \frac{h_1 + h_3}{2}\right)\delta\theta \tag{39}$$

Making the further assumptions that

E) *without loss of generality,* $\delta s = 0$ *at* $\theta = 0$

F) *angles are small, so that* $\theta = dw/dx$

it follows that the shear strain γ in the rubber is given by

$$\gamma = \frac{s}{h_2} = \left(1 + \frac{h_1 + h_3}{2h_2}\right)\frac{\mathrm{d}w}{\mathrm{d}x} \tag{40}$$

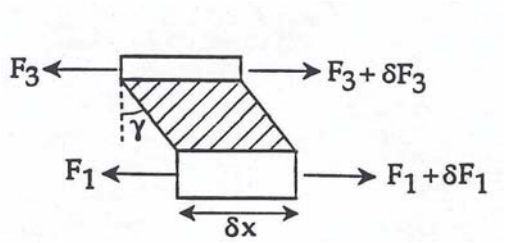

Figure 7: Element of laminar beam used to derive relationships between shear in the rubber and axial forces in the shims

The shear tractions applied by the rubber results in axial forces per unit width tending to extend or compress the shims. From Fig. 7, it is apparent that

$$\begin{aligned} \frac{\mathrm{d}F_3}{\mathrm{d}x} &= -G\gamma \\ \frac{\mathrm{d}F_1}{\mathrm{d}x} &= G\gamma \end{aligned} \tag{41}$$

Under the action of forces F_1 and F_3 the shims will change length, in conflict with assumption

(C). For the present simplified theory to be valid, a criterion is required for the condition that these changes in length are negligible.

Considering the element of length δx depicted in Fig. 7, we find the axial strains in the shims relieve the shear strain in the rubber according to

$$\frac{d\gamma}{dx} = \left(\frac{F_1}{E_1 h_1} - \frac{F_3}{E_3 h_3}\right)\frac{1}{h_2}$$

Differentiating and applying Eq. (41) gives

$$\frac{d^2\gamma}{dx^2} = \frac{G}{h_2}\left(\frac{1}{E_1 h_1} + \frac{1}{E_3 h_3}\right)\gamma \equiv \beta^2\gamma \qquad (42)$$

The solution of Eq. (42), if there is no more bending, is

$$\gamma = \gamma_0 \exp(-\beta x) \qquad (43)$$

The constant $1/\beta$, where β is defined in Eq. (42), has been termed the "shear length" [Kerwin & Ungar, 1990]. The criterion for validity of assumption (C) – lack of extension of the metal layers – is thus

$$L^2\beta^2 << 1 \qquad (44)$$

where L is the length of the laminate.

Two further assumptions are made to complete the theory for flexure of the laminate:

G) *the axial force in the rubber layer is negligible*

H) *the bending moment applied to the rubber layer is negligible*

5.3 *Differential equation for the profile of a laminar beam subject to end loadings only*

It follows from the assumptions developed in section 5.2 and consideration of Fig. 8 that

$$M = \frac{F_3(h_2+h_3) - F_1(h_2+h_1)}{2} + M_3 + M_1 \qquad (45)$$

The constitutive laws for the moments in the shims are taken from simple beam theory:

$$\text{constitutive law for shims } M_i = \frac{E_i h_i^3}{12}\frac{\mathrm{d}^2 w}{\mathrm{d}x^2} \qquad (46)$$

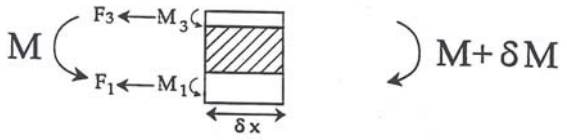

Figure 8: Contribution of the separate layers to the overall bending moment M in the composite beam. M_2 and F_2 are assumed to be negligible

Differentiating Eq. (45), and making use of Eqs. (46), (40) and (41) leads to the differential equation for the composite beam:

$$\frac{\mathrm{d}M}{\mathrm{d}x} = \tilde{k}\frac{\mathrm{d}^3 w}{\mathrm{d}x^3} - \tilde{h}^2\frac{G}{h_2}\frac{\mathrm{d}w}{\mathrm{d}x}$$
$$\text{where } \tilde{k} = \frac{E_1 h_1^3 + E_3 h_3^3}{12} \text{ and } \tilde{h} = h_2 + \frac{h_1+h_3}{2} \qquad (47)$$

$\tilde{k}$ is the combined bending stiffness per unit width for the shims.

Problems involving flexure of beams under the action of a shear force Q and axial force P may be solved by using Eq. (47) in conjunction with the usual moment equilibrium equation from simple beam theory, obtained by differentiating the analogue of Eq. (20):

$$\text{static equilibrium condition } \frac{\mathrm{d}M}{\mathrm{d}x} = -Q - P\frac{\mathrm{d}w}{\mathrm{d}x} \qquad (48)$$

The profile adopted by the laminar beam is not a cubic polynomial as for simple beam theory (for the case that P = 0) but can be expressed in terms of hyperbolic functions $\cosh(\alpha x)$ and $\sinh(\alpha x)$ where

$$\alpha^2 = \frac{G}{h_2}\frac{\tilde{h}^2}{\tilde{k}} \qquad (49)$$

The dimensionless quantity αL, where L is the length of the beam between point loads, is a measure of the relative contributions of rubber, as opposed to shims, in controlling the profile. For large values of αL the shape of the deformed laminar beam consists of relatively straight lines between the supports. In consequence, in the case

of a 3-point bend test there is no deflection in the overhang region (Fig. 9), in contrast to the case for a conventional beam. Experimental determinations of the behaviour of such laminar beams are in accord with the theory [Muhr & Thomas, 1989].

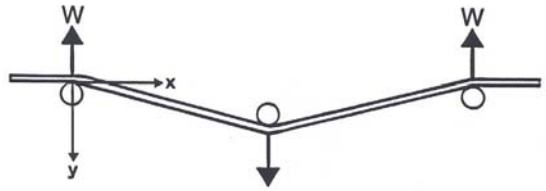

Figure 9: Three-point bend test of a laminar beam with a large value of αL; note there is no deflection in the overhang region [Muhr & Thomas, 1989]

6 Wrinkling Instability of Flexible Shims Bonded to Rubber

The dominant mechanism of failure of laminates with thin shims bonded to a thick rubber core was found in experimental work to initiate with wrinkling of one metal layer if the overall deformation became sufficiently large [Muhr & Thomas, 1989]. If the laminate was flexed further, the shim would buckle at the locus of the wrinkles and collapse. It appears that the compressive force applied by the sheared rubber to the metal results in an elastic instability similar to that for an Eulerian strut. This section provides the details of the derivation promised by Muhr & Thomas [1989]

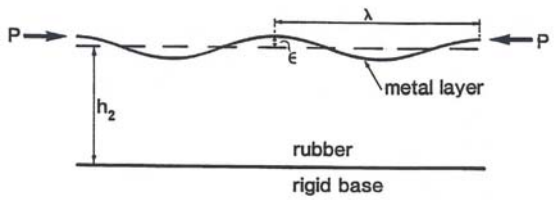

Figure 10: Wrinkle in a shim bonded to a layer of rubber and subjected to a compressive force P

The threshold of elastic instability can be calculated in the following way. A compressive force P per unit breadth (calculable, for example, from integration of Eq. (41)) is assumed to act on the shim causing it to deform into a sinusoidal ripple of amplitude ε and wavelength λ (see Fig. 10). The changes in energy per unit breadth, plane strain being assumed throughout, accompanying this deformation are:

1) *The force P moves through a distance* Δ *and thus does work P* Δ. The distance Δ may be calculated by assuming the centre line of the shim does not change in length, thus

$$\Delta = \int_0^\lambda \sqrt{1+\left(\frac{\mathrm{d}v}{\mathrm{d}x}\right)^2}\,\mathrm{d}x - \lambda \tag{50}$$

where $v = \varepsilon\cos(2\pi x/\lambda)$,
whence $\Delta = \frac{\varepsilon^2\pi^2}{\lambda} + O(\varepsilon^4)$
Here x is the coordinate parallel to the surface and y the coordinate normal to it.

2) *The flexure of the shim causes elastic energy to be stored in it.* This energy may be calculated as:

$$U_M = \frac{1}{2}k\int_0^\lambda \left(\frac{d^2v}{dx^2}\right)^2 dx = \frac{4\pi^4 k\varepsilon^2}{\lambda^3} + O(\varepsilon^4) \tag{51}$$

where $k = Et^3/12$, t being the thickness of the shim.

3) *The rubber is bonded to the shim so that it becomes wrinkled on its surface, storing elastic energy in the bulk.* Observations suggest that the wrinkles are confined to one metal layer, the other layer remaining relatively flat. We shall assume that the energy associated with lateral compression is negligible, and equate the stored energy to the work done by the tractions normal to the rubber surface as the wrinkle forms:

$$U_R = -\frac{1}{2}\int_0^\lambda \sigma_y\varepsilon\cos(2\pi x/\lambda)\mathrm{d}x \tag{52}$$

where σ_y is the stress normal to the surface of the rubber. The value of σ_y is determined by first finding the stress function $\phi(x,y)$ which must, for compatibility with a continuous strain field, satisfy

$$\frac{\partial^4\varphi}{\partial x^4} + 2\frac{\partial^4\varphi}{\partial x^2\partial y^2} + \frac{\partial^4\varphi}{\partial y^4} = 0 \tag{53}$$

and in terms of which the stresses may be found:

$$\begin{aligned}\sigma_x &= \frac{\partial^2\phi}{\partial y^2}\\ \sigma_y &= \frac{\partial^2\phi}{\partial x^2}\\ \tau_{xy} &= -\frac{\partial^2\phi}{\partial x\partial y}\end{aligned} \tag{54}$$

and hence, using the generalized Hooke's law, the strains may also be found:

$$\begin{aligned}\frac{\partial u}{\partial x} &= \frac{1}{4G}(\sigma_x-\sigma_y)\\ \frac{\partial v}{\partial y} &= \frac{1}{4G}(\sigma_y-\sigma_x)\\ \frac{\partial u}{\partial y}+\frac{\partial v}{\partial x} &= \frac{1}{G}\tau_{xy}\end{aligned} \tag{55}$$

To satisfy the boundary conditions that $u=0$, $v=\varepsilon\cos(2\pi x/\lambda)$, $t_{xy}=0$ on $y=0$; $u=0$, $v=0$ on $y=h_2$, it turns out that:

$\varphi(x,y)=\varepsilon C\cos(2\pi x/\lambda)f(y)$ where

$$\begin{aligned}f(y)=&\left[1+\frac{2\pi y}{\lambda}\tanh\left(\frac{2\pi h_2}{\lambda}\right)\right]\cosh\left(\frac{2\pi y}{\lambda}\right)\\ &-\left[\frac{2\pi y}{\lambda}+\tanh\left(\frac{2\pi h_2}{\lambda}\right)\right]\sinh\left(\frac{2\pi y}{\lambda}\right)\end{aligned} \tag{56}$$

and $C=\dfrac{G\lambda\cosh\left(\frac{2\pi h_2}{\lambda}\right)}{\pi\left[\sinh\left(\frac{2\pi h_2}{\lambda}\right)-\frac{2\pi h_2}{\lambda}\right]}$

whence we find

$$U_R=\frac{\pi^2 C\varepsilon^2}{\lambda} \tag{57}$$

Finally, the criterion for wrinkling is

$$P\Delta \geq U_M+U_R \tag{58}$$

Wrinkling will occur with a wavelength such that the inequality is satisfied for a minimum value of P. This critical value of P is found from the condition that dP/dλ = 0. Although differentiation can be carried out analytically, the resulting equation was solved numerically for λ. Substitution of this value of λ back into Eq. (58), written as an equality, yields the critical value of P. The value of λ_∞ for $h_2\to\infty$ provides a good starting point for the numerical iteration:

$$\lambda_\infty = 2\pi\left(\frac{k}{G}\right)^{\frac{1}{3}} \tag{59}$$

The corresponding critical value of P is

$$P_\infty = 3\left(kG^2\right)^{\frac{1}{3}} \tag{60}$$

Experiments were carried out for comparison with this theory [Muhr & Thomas, 1989]. Laminates with extra thick metal back layers were made and deformed as shown in Fig. 11. The deflection at which wrinkling was observed was measured; the theory can be used to predict this deflection, from knowledge of G, h_2 and k. The results, shown in Fig. 12, are in good agreement with the theory.

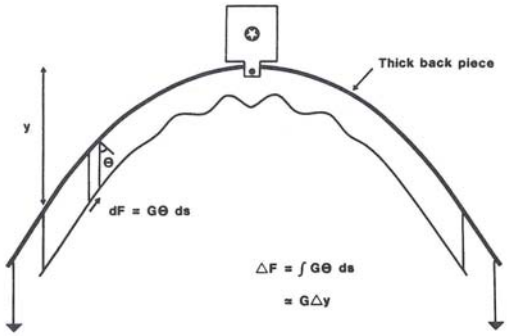

Figure 11: Arrangement for determining the wrinkling force.

7 Finite Element Analysis (FEA) of Elastomer-Shim Laminates

The laminated structure may be modelled in detail, the discrete materials being modelled explicitly, with all material interfaces falling along element boundaries [eg Gregory & Muhr, 1995]. Alternatively, an equivalent homogeneous material may be devised which captures the overall anisotropic behaviour of the composite, but will not deliver details of the local strains in each material without post processing of the large scale

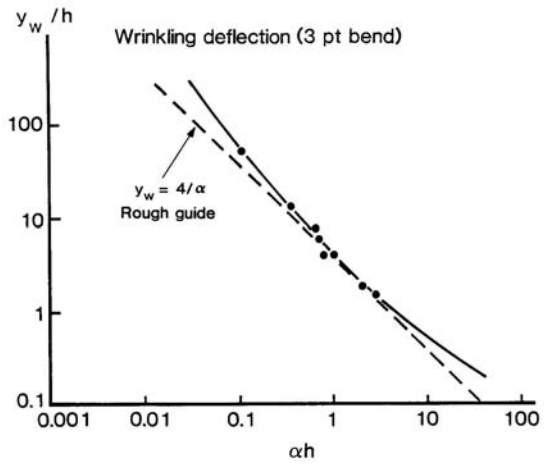

Figure 12: Comparison between experimental wrinkling results and the prediction of equation (58)

variables [Herrmann & Lim, 1984]. The second approach resembles that of the beam-column theory discussed above, in that the mechanical properties are "smeared" out to give an equivalent continuum description, but has the advantage, through the FE method, of extension to more complicated geometry, nonlinear responses and less restrictive assumptions. By reducing the number of elements required, it offers considerable saving in CPU time over the discrete approach, but requires four extra degrees of freedom to capture the local deformation.

The equivalent homogeneous modelling of elastomer-shim laminates of Herrmann, Hamidi, Shafigh-Nobari & Lim, [1988] will now be summarised.

The composite is characterised by choosing the normal to the shims to coincide with one coordinate axis (eg a Cartesian axis, say z, for flat shims), and by specifying the thicknesses, say h_s and h_f for the stiff and flexible layers respectively, and the elastic properties of the two materials.

The equivalent homogeneous continuum model used for FEA of the composite is not a conventional orthotropic model, but specially developed to enable the unusually large scale of the effects of free edges to be modelled. In contrast to the case for other laminates, the scale of penetration of these effects from the free edges greatly exceeds the thickness of the layers, because of the very high ratio of the moduli of rigidity, together with the high ratio of bulk to shear moduli of elastomers. This is similar to the point made by Spencer [1972] for cord-rubber composites: the shims can channel stress from one point to a far distant point, in conflict with St Venant's principle.

Deformation of the composite is defined by an augmented set of seven global degrees of freedom u, v, w, δ_x, δ_y , ϕ_x, ϕ_y. The first three variables are the "smeared" displacements at any point, equivalent to the actual values at the centres of the shims, but defined by interpolation elsewhere. They are not sufficient to calculate local strains in each material, but need to be augmented by the variables δ_x, δ_y that quantify the averaged bulge of the elastomer relative to the shims between which it is sandwiched. In addition, the variables ϕ_x, ϕ_y are needed to quantify the rotation of the embedded normal in the shim, capturing the tendency of the shims to bend and shear, especially important near to free edges when the laminate is sheared. Variables u, v, w, ϕ_x, ϕ_y only have physical meaning at the centres of the shims, but the "smeared" nature of the equivalent homogeneous composite model treats them, as well as δ_x, δ_y, as continuously variable.

Unlike the simple linear interpolation of the seven global variables across a representative volume element, the actual material displacement fields have complicated dependences, expressed in terms of local scales and values of the global variables at reference positions, taking into account plate theory for the shims and equations such as those of section 2 for the elastomer. The theory also includes three coefficients, which, for the linear case, can be expressed in terms of the seven global variables, but for the non-linear case are treated as additional unknowns, to be determined for each element. Equations for local strains in terms of the seven global variables and three coefficients were derived, and from these the total deformation energy can be calculated and used in the principle of minimum potential energy for equivalent homogeneous FEA of the elas-

tomer shim composites.

Herrmann, Hamidi, Shafigh-Nobari & Ramaswamy [1988] describe the implementation of the equivalent homogeneous composite model in FEA and compared results with discrete FEA and experiment. They concluded that the "theory is an accurate and computationally efficient analysis tool". Further FE predictions based on the theory were presented by Herrmann, Ramswamy & Hamidi [1989]. They included the effect of shim stiffness on axial stiffness of the bearings, and the effect of axial load on the shear load-deflection behaviour. However, the influence of shim flexibility on the latter was not addressed.

8 Discussion

The body of knowledge on mechanical properties of rigid shims has not been exhausted by the brief account in this paper. As well as solutions for the nearly incompressible case, the literature provides solutions for flat rectangular laminates, flat elliptical laminates and flat cylindrical laminates with central holes [see reviews by Gent, 1994 and Yeoh, 2002]. Cylindrical bushes present yet another geometry that has been solved by Ritz-type methods [eg Busfield & Davies, 2001; Horton, Gover & Tupholme, 2000]. All these geometries and accompanying stiffness equations have been developed to provide engineering components whose stiffness matrices can be tailored to suit particular applications, calling for highly anisotropic stiffnesses.

There is also some literature addressing nonlinear load-deflection behaviour, which as seen in section 3.2 is significant for forces or moments resulting in change of thickness of the rubber layers. Clearly the tangential stiffness must become unbounded as the shim spacing reduces to zero, and a rough way of taking this into account is to calculate the shape factor on the basis of the current shim separation, rather than the load-free separation [Lindley, 1966].

The theory for flexible rubber-shim laminar beams has been motivated by exploitation of rubber to impart damping to steel panels [Kerwin & Ungar, 1990], as well as by the possibility of using such structures as “rubber” springs [Muhr & Thomas, 1989]; many of these publications focus on the partition of the deformation energy between rubber and shims.

Instability is also associated with enhanced damping [Thomas, 1983; Coveney, Muhr & Thomas, 1989; Goodchild & Thomas, 2007], since deformations applied at instability are accompanied by the usual energy dissipation for the rubber, but the storage stiffness and hence energy is zero, so the ratio of the energies (the apparent loss factor, a measure of damping) has a singularity. This feature could perhaps be exploited, in combination with the high strength capability of microcomposites, to produce composite materials with enhanced damping.

Strength enhancement of microcomposites is believed to derive from the impossibility of flaws, in each phase, being greater than the scale of heterogeneity. Even for effectively long interlaminar cracks there is an effect of scale normal to the interlaminar crack growth direction, as is apparent from Eq. (38).

Cord – rubber composites share some of the characteristics of laminates of rubber with flexible shims. However, the in-plane extensional stiffness of a plane formed by sets of cords plied at a bias angle is not isotropic, being very high in line with any set of cords and much lower in other directions. Instabilities akin to the wrinkling of shims can occur if the cord-rubber composites are subjected to excessive flexure. Glass fibre cords are less robust in such circumstances than other types of cord, and are not suitable as reinforcement, for example, for tyres subjected to kerbing.

9 Conclusions

A comprehensive body of theory is available for relating the strongly anisotropic mechanical properties, the local stresses, energy release rates and damping of rubber-shim composites to their detailed geometry.

As for the theory of cord-rubber composites, the detailed theory gives a better description and more insight than fitting parameters to an anisotropic continuum model for the composite. The Ritz

method has been useful to this end but only in some cases has it been worked beyond provision of good approximations, to give rigorous upper bound stiffnesses.

Specific solutions of the detailed theory provide useful benchmarks for approximate numerical modeling techniques for related composites.

FEA, whether based on the detailed structure or an appropriately smeared composite, can be used to predict behaviour in situations not accessible to existing theory, such as non-linearity of load-deflection behaviour.

Failure mechanisms analysed for rubber-shim composites may give insight into failure mechanisms for other composite materials with cord-like or shim-like inclusions.

Acknowledgement: are due to K L Johnson for suggesting the method of deriving the criterion for wrinkling of shims (section 6), to R A Schapery for providing stiffness equations for section 2.3, and to J. Gough for checking parts of the manuscript.

References

Adkins, J.E. (1954) Some generalisations of the shear problem for isotropic incompressible materials. *Proc. Camb. Phil. Soc.* , vol 177, pp 334-345.

Ahmadi H.R. & Muhr A. H. (1997) Modelling the dynamic properties of filled rubber. *Plastics, Rubber & Composites,* vol. 26, pp 451 – 461.

Bauman J.T., Calculation methods for spherical elastomer bearings, Part III: Torsion. Paper 68 at ACS Rubber Division Meeting, San Antonio, May 2005

Busfield, J.J.C. & Davies, C.K.L. (2001), Stiffness of simple bonded elastomer bushes. Part 1 – Initial behaviour. *Plastics, Rubber & Composites*, vol. 30, pp 243-257.

Chalhoub M.S. and Kelly, **J.M.** (1990) Effect of bulk compressibility on the stiffness of cylindrical base isolation bearings, *Int J Solids Structures*, vol. 26, pp 743 – 760,

Coveney, V.A., Fuller K.N.G & Muhr A.H., (1989) Stresses developed in rubber/concrete contact,s. In *Contact Stress Mechanics.* IOP short Meeting no. 25, ed A.D.Roberts & J.E.Mottershead, publ IOP.

Coveney V.A., Muhr A.H. and Thomas A.G., (1989) Damping behaviour in flexible laminates, *Damping '89 Proceedings,* West Palm Beach, Florida, Publ. Flight Dy-namics Laboratory.

Gent, A.N. (1964) Elastic stability of rubber compression springs, *J.Mech. Engrg. Sci*. .,vol 6, pp 318-326,

Gent, A.N. (1994) "Compression of rubber blocks" *Rubber Chem & Technol*, vol. 67, 549 – 558.

Gent, A.N., Henry R.L. & Roxbury M.L., (1974) "Interfacial stresses for bonded rubber blocks in compression and shear", *J. Appl. Mech.,* vol. 41, pp 855 -859.

Gent A.N. and Lindley P.B., (1959) The compression of bonded rubber blocks. *Proc. Instn. Mech. Eng.* vol. 173, pp 111- 117,

Gent A.N. and Lindley P.B., (1958) Internal rupture of bonded rubber cylinders in tension, *Proc. Roy. Soc.* A249, pp 195-205.

Gent A.N. and Meinecke, **E.A.** (1970) Compression, bending and shear of bonded rubber blocks *Polymer Eng & Sci* vol 10 pp 48-53

Goodchild I.H & Thomas A.G., (2007) Lateral stiffness and damping of a stretched rubber beam. *J.Polym. Sci. B Polym. Phys.* (submitted)

Gough J. and Muhr A.H., (2005) Initiation of failure of rubber close to bondlines, *Proc International Rubber Conference,* Maastricht, June 2005

Gregory I.H. and Muhr A.H., (1995) Design of elastomeric anti-seismic bearings, In *European Seismic Design Practice,* pp 479 – 486, ed. Elnashai, publ. Balkema.

Gregory I.H. and Muhr A.H., (1999) Stiffness and fracture analysis of bonded rubber blocks in simple shear. In: *Finite Element Analysis of Elastomers*, D. Boast & V.A. Coveney (eds.), Professional Engineering Publishing, pp 265-274.

Herrmann L.R., Hamidi R., Shafigh-Nobari F. & Lim C.K., (1988) Nonlinear behaviour of elastomeric bearings. I Theory. *J Eng Mechanics*, vol.

114 pp 1811-1829

Herrmann L.R. & Lim C.K, (1984) Equivalent homogeneous FE model for elastomeric bearings. *J Eng Mechanics*, vol. 113 pp 106-125

Herrmann L.R, Hamidi R, Shafigh-Nobari F. & Ramaswamy A. (1988) Nonlinear behaviour of elastomeric bearings. II FE Anlaysis and verification. *J Eng Mechanics*, vol. 114 pp 1831-1853

Herrmann L.R., Ramswamy A. & Hamidi R., (1989), An analytical parameter study for a class of elastomeric bearings. *J. Structural Eng*, vol 115, pp 2415 – 2434

Horton, J.M., Gover, M.J.C. & Tupholme, G.E. (2000), Stiffness of rubber bush mountings subjected to tilting deflection. *Rubber Chemistry & Technology*, vol. 73, pp 619-633.

Kelly J.M., (1994) The influence of plate flexibility on the buckling load of elastomeric isolators, Report UCB/EERC-94/03, University of California at Berkeley.

Kerwin E.M. and Ungar E.E., (1990) Requirements imposed on polymeric materials by structural damping applications, Ch.17 in *Sound and Vibration Damping with Polymers*, ed. R.D.Corsaro and L.H.Sperling, publ. ACS.

Lindley P.B., (1966) Load-compression relationship of rubber units. *J. Strain Analysis,* vol. 1, pp 190-195

Lindley P.B. and Teo S.C. (1979) "Energy for crack growth at the bonds of rubber springs" *Plastics & Rubber: Materials and Applications*, vol 4, pp 29-37,

Muhr A.H. and Thomas A.G., (1989) Flexible rubber-steel sandwich springs, *Rubber Chem. Tech*., vol 62, pp 820 - 837.

Muhr A.H. and Thomas A.G., (1991) Design of laminated elastomeric bearings for base isolation, *Proc Int. Meeting on Earthquake Protection of Buildings*, Ancona, Italy, Publ. CREA.

Papoulia K. & Kelly J. M., (1996) Compression of bonded blocks of soft elastic material: variational solution. *J. Eng Mechancis,* vol. 122, pp 163 - 170.

Rocard, Y. (1937) Note sur le calcul des propriétés elastique des supports en caoutchouc adhérent. *Journal de Physique et de Radium,* vol 8, pp 197-203.

Schapery R.A., and Skala D.P., (1976) Elastic stability of laminated columns, *Int J. Solids Structures*, vol 12, pp 401 – 417.

Schapery R.A., (2006) private communication regarding company reports, eg ref 7 of Schapery & Skala (1976).

Spencer, A.J.M. (1972) *Deformations of fibre-reinforced materials.* Oxford Science Research Papers, Clarendon Press, Oxford**.**

Stanton, J.F., Scroggins, G, Taylor, A.W & Roeder, C.W., (1990) "Stability of laminated elastomeric bearings", *J. Eng. Mech,* vol. 116, pp 1352 – 1371.

TARRC (1979 – 1986) Engineering Data Sheets.

Thomas A.G., (1983) The design of laminated bearings, *Proc. Int. Conference on Natural Rubber for Earthquake protection of Buildings*, ed. C.J.Derham, Publ. MRRDB, Kuala Lumpur.

Timoshenko S.P. and Goodier, J.N. (1970) *Theory of Elasticity*, McGraw-Hill, 3rd Edition.

Yeoh, O.H. (1985) The Compression of tall rubber cylinders", *J Rubber Research Inst Malaysia,* vol. 33, pp 109 - 114.

Yeoh, O.H. (2002) "Compression of bonded rubber blocks", *Rubber Chem and Tech.,* vol. 75, pp 549-561.